Supplement

S1. Control of viscosity ratio on the dynamic pressure inside wedge

The corner flow theory presented in the main text (section 4.3, Fig. 1c, 12) suggest that a wedge generates a dynamic pressure (P_d) field at its narrowing end, which serves as the driving force for the characteristic return flow. In tectonic settings with slab-parallel subduction, high dynamic pressures localize preferentially at the base of the wedge and its overriding wall, as shown in Figure S1. Our generalized corner flow model predicts a positive correlation of the P_d magnitude with the viscosity ratio (μ_r) between the overriding plate (OP) and the wedge, increasing consistently as μ_r rises. The dynamic pressure gradient across the wedge tends to deflect part of the return flow towards the wall. At μ_r =10, the system hardly generates any P_d -gradient along the wedge (Fig. S1 c), and the corner flow is mostly deflected towards the overriding wall (Fig. 4c in the main text).

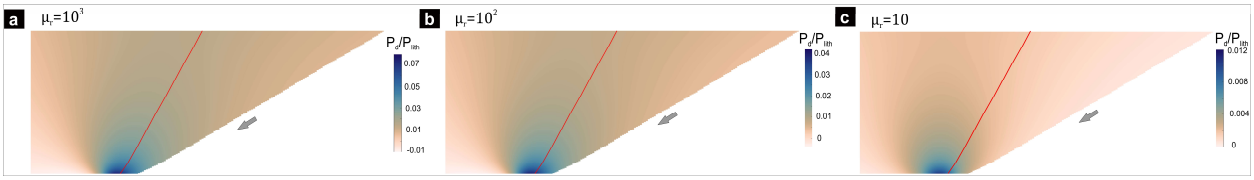

Fig. S1: Plot of normalized dynamic pressure (P_d) with varying μ_r. Arrows indicate slab-parallel subduction direction. $\mu_l = 10^{19}$ Pa s. $\theta_l = 30°$, and $d = 30°$.

Slab advance motion during subduction contributes to the buildup of additional dynamic pressure at the base of the wedge and along the wall (Fig. S2 a-i, ii). For moderate μ_r (= 10^2), such a pressure field sets in return flows in both the wedge and its wall (Fig. 5d-i in the main text). In contrast, slow slab rollback ($\phi < \sim 2\theta_l/3$ or rigid OP) generates negative P_d due to bulk extension across the wedge, which counteracts the positive P_d produced by the wedge's taper geometry. Ultimately, the wedge fails to develop any significant dynamic pressure in a slab-rollback subduction setting (Figure S2 b-i, ii). Large slab rollback rates ($\phi > \sim 2\theta_l/3$) lower dynamic pressure to become completely negative (Figure S2 b-i, ii). Such negative pressures 'draw in' the wedge materials towards the bottom in facilitating the burial of wedge materials at high rates, which locally exceed the subduction velocity (see Fig. 5c-i, f-i in the main text).

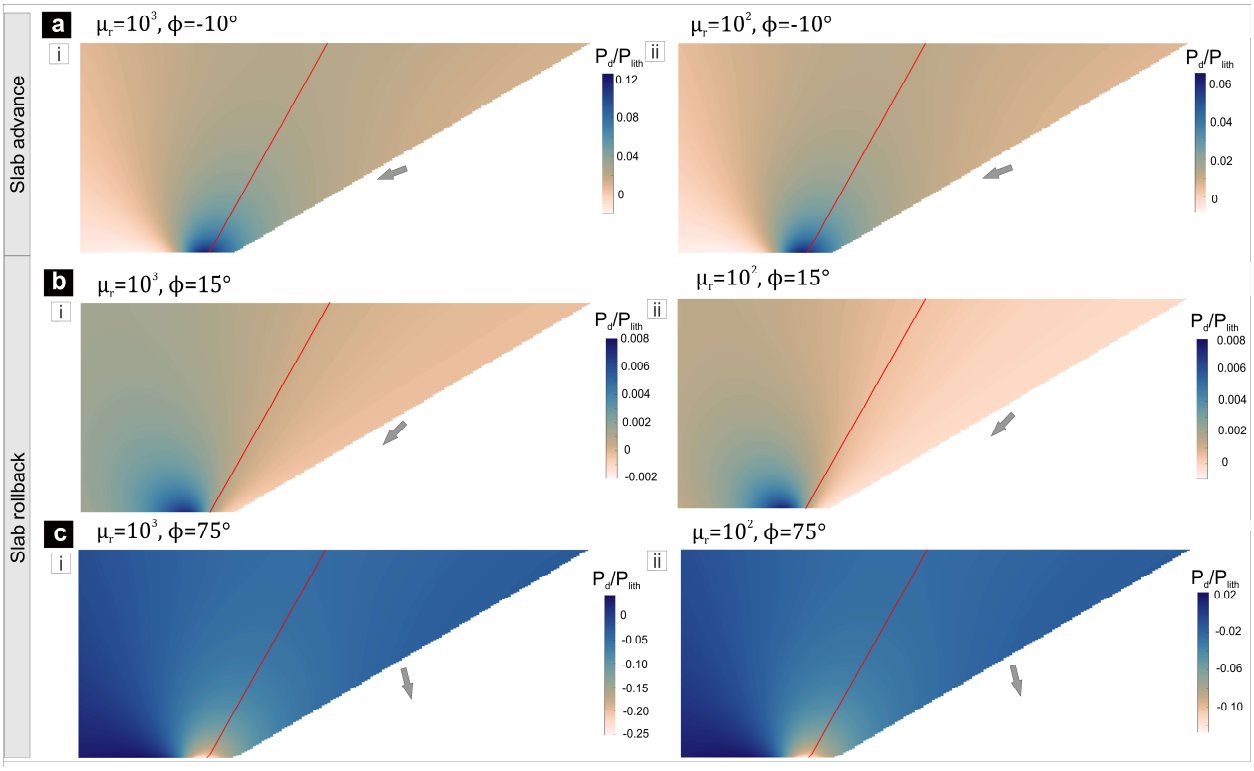

Fig. S2: Plot of normalized dynamic pressure (P_d) as a function of ϕ, and μ_r. μ_l = 10^{19} Pa s. θ_l = 30°, and d = 30°. P_{lith} is calculated assuming the overburden density as 2800 kg/m3.

S2. Laboratory model experiments: velocity boundary conditions

The laboratory model setup consisted of three rigid buttresses, driven by two step-up motors, used differently in different sets of experiments to simulate shearing, oblique shortening and oblique extension within the wedge (see Fig. 9 of the main text). For shearing, buttress 1 was driven to pull a plastic sheet along the wedge base at a rate of 4 mm/min. In another set of experiments, the plastic sheet had an along-base velocity (3.8 mm/min), coupled with a horizontal movement of buttress 2 that produced an across-wedge shortening velocity (1.24 mm/min). The two motions together simulated a condition of oblique shortening at an angle (ϕ = -18°) to the wedge base. For the third set of experiments, a basal buttress, attached to buttress 1, was placed at the base of the deformable wall (Figure 9 of the main text). This model configuration allowed the buttress 1 to tangentially move the plastic sheet along the wedge base, as well as the deformable wall to move away from the wedge. This kinematic setup replicates an oblique subduction kinematics with the movement direction at an angle to the wedge base (ϕ =

68°) away from the deformable wall in a reference frame fixed to the basal buttress. The velocity boundary conditions of the different sets of experiments are summarized below in Table S1.

Table S1. Imposed velocity boundary conditions for different sets of experiments.

Experiment	Buttress 1	Buttress 2	Basal buttress
Shearing	4 mm/min	0	0
Oblique shortening	3.8 mm/min	1.24 mm/min	0
Oblique extension	2.16 mm/min	0	2.16 mm/min